We are IntechOpen,
the world's leading publisher of
Open Access books
Built by scientists, for scientists

6,900
Open access books available

185,000
International authors and editors

200M
Downloads

154
Countries delivered to

Our authors are among the

TOP 1%
most cited scientists

12.2%
Contributors from top 500 universities

CLARIVATE ANALYTICS
BOOK CITATION INDEX
INDEXED

WEB OF SCIENCE™

Selection of our books indexed in the Book Citation Index
in Web of Science™ Core Collection (BKCI)

Interested in publishing with us?
Contact book.department@intechopen.com

Numbers displayed above are based on latest data collected.
For more information visit www.intechopen.com

Ion Implantation as a Tool for Controlled Modification of Photoelectrical Properties of Silicon

Nina Khuchua, Marina Tigishvili, Nugzar Dolidze,
Zurab Jibuti, Revaz Melkadze and Roland Diehl

Additional information is available at the end of the chapter

Abstract

The results of our recent studies of controlled modifications of the photoelectrical properties of n-Si due to B^+ ion implantation are supplemented with new data, summarized and analyzed. The starting material was wafers of single-crystalline n-Si and a silicon-on-insulator structures. p-n-Si structures were fabricated by ion implantation of B^+ in doses ranging from 1×10^{13} to 1×10^{15} cm^{-2} and ion acceleration energies of 50 and 32 keV. Subsequent annealing was performed both by steady-state (900 and 1000°C, 20 min) and pulsed photon processing. In such structures, a pronounced photosensitivity is observed in the short-wave infrared range (1.5–2.2 μm), as well as in the ultraviolet region within 0.25–0.40 μm. A well-defined correlation between the structural, electrical and photoelectrical properties and the implantation and annealing regimes, as well as the content of C and O impurities is demonstrated. In the starting material, a damaged layer with a thickness of hundreds of nanometers was found to have a significant effect on the results obtained. The main results are discussed in terms of the formation/transformation of deep-level extended defects in n-Si during B^+ implantation followed by annealing. Innovative application approaches of the technology are obvious.

Keywords: single-crystalline n-Si, damaged near-surface layer, boron ion implantation, annealing regimes, p-n-Si structures, IR and UV photosensitivity, C and O impurities, deep level extended defects

1. Introduction

Studies of the optical and photoelectric properties of semiconductors are in most cases equivalent with respect to their scientific and practical significance. The first aims at a thorough

understanding of the processes involved in a particular material behavior under the influence of electromagnetic radiation (EMR). The second is due to the variety of EMR semiconductor converters used in various fields of technology.

Apart from a more classical point of view which looks at the sensitivity of a semiconductor to various regions of the EMR spectrum depending on the bandgap, materials the initial fundamental properties (structural, electrical, optical) of which are modifiable due to the specific impact of technological processes [1] are of ever increasing interest.

The classical approach cannot solve all the problems that arise when developing detector/sensor systems, e.g. for specific ranges of the infrared (IR) and ultraviolet (UV) spectra. Therefore, new technologies are emerging, in particular the so-called defect engineering. Applying this scientific-technical approach, a number of fundamental semiconductor characteristics are changed due to purposefully creating a variety of defects that modify the material properties. The effective behavior is sometimes difficult to understand - the practical result can be observed immediately, whereas its interpretation turns out to be rather complicated requiring quite a number of various tools and methods of investigation and characterization.

A very attractive and promising material for a variety of applications with respect to modifying its properties is unipolar silicon with its high level of processability and easy availability.

Because silicon is transparent for wavelengths exceeding 1.1 µm, it cannot be used directly e.g. for the development of IR photodiodes. One of commonly applied methods to obtain various structural modifications, is changing the width of the Si bandgap using Ge. Most efficient structures are grown by molecular beam epitaxy (MBE).

In [2], it was shown that, when single crystalline Si is subjected to electropulse treatment, the self- absorption edge of the material shifts to 1.33 µm. This is undoubtedly referred to a change in the band structure of Si allowing for bandgap engineering, but so far the practical application potential of the technology is unclear.

In some cases, ion implantation (II) can be considered as an alternative to the MBE method. II enables the materials' researcher and engineer to tightly control the introduction of impurities into the semiconductor, creating a variety of defects the type, concentration and electrical activity of which are largely determined by the conditions of post-implantation annealing [3, 4]. Altogether, by applying such processes the fundamental properties of the material are changed.

Undoubtedly, this area of technology is not only of scientific but also of practical interest, as it provides access to specific semiconductor electro-optical EMR converters which include detecting devices for various ranges of IR and UV spectra [5, 6].

The II technology is attractive because of its relative simplicity, reproducibility and low-cost potential. However, the physical mechanisms behind the influence of certain defects on the optical and photoelectrical properties of the material are not easily evident. Such defects are not only formed during II, but also transformed by annealing in the subsequent heat treatment process. Therefore, defect engineering requires various techniques to be involved such as Raman and IR spectroscopy, X-ray diffraction, transmission electron microscopy (TEM), photo- and electroluminescence, *deep-level transient spectroscopy* (DLTS), etc.

It is known that in silicon technology, boron is one of the widely used impurities, e.g. for the production of single-crystalline p-type material, creation of p-n junctions, etc. A large number of original papers were published and many overviews articles have been devoted to the study and description of defects formed during ion doping of Si with boron (see [7–11], etc.). In general, it is shown that applying the process of II, a wide range of defects is formed, which, due to annealing, evolve from point-like to complex extended defects. For light ions (such as boron) implanted into single-crystalline silicon, for each set of dose-annealing conditions a special type of defects predominate [4].

In [4, 12] it is concluded that the formation of residual extended defects in silicon needs an dose "threshold". This means that such structural disorder during heat treatment (at least 700°C) arises only if a critical concentration of point defects has accumulated. For boron ions with energies of 10–100 keV this occurs at doses of the order of 1×10^{14} cm^{-2}.

It was found that most point defects in Si are annealed at temperatures up to 450°C [4, 7].

Extended defects formed at elevated temperatures are preserved, according to different data, up to an annealing temperature of 1000°C and beyond [15, 16]. In [10], during B$^+$ implantation with different acceleration energies (10–80 keV) and annealing at 950°C, sufficiently large (30–200 nm) dislocation loops were detected by TEM. It is shown that the acceleration energy does not only affect the depth, but also the size and density of these defects. When introducing B$^+$ ions with an energy of 75 keV, dose 1×10^{15} cm^{-2} and annealing at 700°C, only defects of the road-like {311} were detected by TEM. By increasing the temperature further, these defects are transformed into dislocation loops [11].

In defect formation not only introduced but also unavoidable impurities take part. Oxygen and carbon are one of the main accompanying impurities in Czochralski grown Si crystals The carbon content is estimated to be 5×10^{16} to 2×10^{17} cm^{-3} and the oxygen content was found to be 2.5×10^{17} to 2×10^{18} cm^{-3} [4, 13].

Altogether, the presence of carbon and oxygen is directly related to the defects formed in n-Si ion-implanted with impurities such as B since the content of impurities and inhomogeneities in the substrate significantly affects the migration of defects induced by II as well as their further evolution.

In the framework of this research, defects with deep levels (DL) are of primary interest.

The analysis of the DL spectrum in the silicon bandgap allows us to conclude that there is no clear correlation between these levels and specific structural defects [14, 15]. In addition, different defects can have very similar or even identical values of the DL activation energy.

Finally, we could not find any information on photosensitivity spectra of boron-implanted silicon, especially in the infrared spectral range. Only sparse data is known on the research of IR and UV photosensitivity in B- and As-implanted Si [16].

As mentioned above, data are incomplete, results partially contradictory and not fully understood. Nevertheless, we can draw the following conclusions:

1. Over the past several decades, the formation of structural distortions in the process of II and their subsequent arrangement due to annealing have been extensively studied both theoretically and experimentally. Disclosing the characteristics of these distortions helps scientists to understand and model the phenomena, such as the transient-enhanced diffusion of impurities and the formation of extended defects. However, many issues concerning the agglomeration of defects and their further evolution during annealing are still unresolved, in particular how point defects are combined to form more stable and complex structures such as clusters of defects, and how the latter evolve into extended defects.

2. Finally, even less information is available about the mechanism of the influence of various damages on the optical and photoelectrical properties of p-n junctions formed by B implantation into n-type single-crystalline silicon. Although the data on the photo- and electroluminescence spectra are well documented in the literature, the absorption/photosensitivity spectra have been studied less comprehensively and are not associated with any type of defects.

In the present work, an innovative approach to B^+ II into Si as a tool for controlled modification of photoelectric properties of silicon was proposed. Such an approach is both of scientific and practical importance. However, the materials science involved has been less studied so far. The new resolved issues allow one to gain a deeper insight into the processes of defect formation/transformation in p-n structures obtained by B^+ implantation followed by annealing (hereinafter p-n-Si(B) structures). From the application point of view, this opens up new opportunities for the development of IR and UV photodetectors as a part of the silicon technology.

In this article we summarize the results of our studies of the structural, electrical, and photoelectrical properties of p-n-Si(B).The extensive experimental material described earlier [17–22] is supplemented with new data and findings.

2. Experimental

2.1. Formation of p-n-Si(B) structures

p-n-Si(B) structures were formed by ion implantation (implanter Vesuvii 3 M) with different doses of 1×10^{13}, 1×10^{14}, 4×10^{14}, 6×10^{14}, 8×10^{14}, and 1×10^{15} cm^{-2} and acceleration energies of 50 and 32 keV. For the energy 50 keV the projected range, R_p, and range straggling ΔR_p, calculated using stopping and range of ions in matter (SRIM) software, were 0.175 and 0.055 μm, respectively, and for the energy 32 keV – $R_p = 0.120$ μm and $\Delta R_p = 0.052$ μm. Post-implantation annealing was carried out mainly in a steady-state regime in argon atmosphere at temperatures of 900 and 1000°C for 20 min. For comparison, some samples were subjected to pulse photon annealing (PPA). The design of our system allows illumination of the specimen surface with UV light, and of the reverse side with a halogen lamp.

Figure 1 shows a schematic view of the processed p-n structures of two types. In the case of **Figure 1a**, (100) n-Si single-crystalline wafers with resistivity of about 70 or 10 Ohm·cm and

thickness of 250 μm (University Wafer, USA) were used as a starting material. According to **Figure 1b**, the specimens were silicon-on-insulator (SOI) structures with the working layer of single-crystalline 2 μm n-Si with resistivity up to 30 Ohm·cm. The dielectric layer was also 2 μm thick (manufacturer—Ultrasil Corporation, USA).

After B^+ implantation and annealing, a metal composition Ti/Pt/Au (100/100/1000 Å) or Ti/Au (100/1000 Å) was deposited (through a mask or by lift-off photolithography) in the electron-beam evaporation system Temescal. The alloying was performed in the 210 HEATPULSE system at 350°C (15 s). The first type structures (**Figure 1a**) had a continuous reverse contact, and a point contact for the p-type layer. In the SOI structure (**Figure 1b**), both contacts were formed on the active layer. The mesa structure was obtained by wet etching in a fluorine-containing solution using an acid-resistant photoresist mask.

2.2. Specimen characterization techniques

Diagnostics of the structure of the near-surface layers of the initial and ion-doped material was carried out using two-crystal X-ray diffraction on the Dron-4 installation. The first crystal was the studied sample, and the second was the perfect LiF crystal. Diffracted reflection occurred from the lattice plane hkl (531) oriented at an angle of 2°46' to the primary ray. $Co_{k\beta}$ radiation was used for the experiment.

Raman-spectra were recorded by a Raman-microscope (Renishaw) under He-Ne laser excitation with the wavelength λ_{ex} = 632.8 nm. The thickness of the tested layer was about 1.3 μm, and the wave number reproducibility was 0.1 cm^{-1}. For data analysis the software WiRE3.4 was used.

The surface morphology and elemental composition of the structures to a depth of 1 μm was studied on a YEOL ISU-6510LV scanning electron microscope (SEM). This method providing of sensitivity 0.01% and less was used to determine the C and O composition in Si, averaged over the sample surface.

To measure the I-V characteristics of the diodes the semiconductor parameter Analyzer L2–50 was used.

IR reflection spectra were recorded using a Bruker IFS 66 Fourier-spectrometer within the range of 4000–400 cm^{-1} with a resolution of 0.4 cm^{-2} and wave number accuracy of 0.01 cm^{-1}. For spectra processing the software OPUS 5.5 was used.
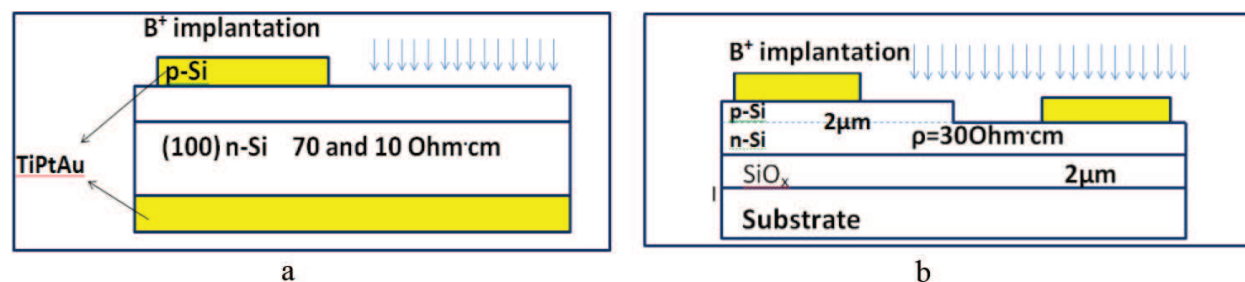

Figure 1. Schematic view of the p-n structures after processing: (a) on n-Si wafers with different resistivity (Si70) and (Si10); (b) on SOI, a, b.

The photosensitivity of the p-n-Si (B) samples in the spectral range 1.0–2.5 µm was measured on a MDR-2 monochromator and IR optical filters.

Since, under real conditions, the photosensitive element is exposed to a beam of light of a limited wavelength range rather than to a non-monochromatic light, we developed a genuine technique and created a setup called "Polychromator," enabling illumination of samples with "packets" of non-monochromatic light. The source of radiation are halogen or mercury lamps, which provide irradiation of samples with light of a wide spectral range (200–4100 nm). This range is regulated by optical filters (altogether 21) selected in such a way that their application allows for varying the spectral ranges by consistently "cutting off" shorter wavelengths.

In our case, the short-circuit current through the element is measured and the quantity

$$\frac{I_n - I_{n+1}}{I_o}, \tag{1}$$

is estimated, where I_o is the current in the sample onto which the entire illumination spectrum is incident, I_n is the current corresponding to the previous filter and I_{n+1} is the current measured for a given particular filter (n = 0, 1, 2, 3, etc.).

Below, the photosensitivity measured by this method will be referred to as "integral" as compared to the data obtained by a monochromator. Such a technique allows one to qualitatively separate the influence of the intensity and spectral composition of the incident illumination on the electrical signal. The value determined by formula (1) may adopt in certain cases a zero or even a negative value.

All measurements were carried out at room temperature, except for the photosensitivity spectra using a monochromator, where the sample was placed into liquid nitrogen.

3. Results

For the samples of both the untreated and boron-implanted silicon with a dose of 1×10^{14} cm^{-2} after stationary annealing (1000°C, 20 min), the diffraction reflection curves were measured. From these curves, the intensity of the diffraction reflection signal, the line half-width, the lattice parameters, the relative lattice deformation, and the interplanar spacing were calculated for each case (**Table 1**).

From the signal line width the degree of crystallinity of the sample structure can be derived: the smaller the width, the more perfect the crystal. On the contrary, a lower intensity of the signal indicates heavy damages of the crystal structure. It is clear that the degree of crystallinity of the ion-implanted and annealed material deteriorates as compared with the untreated one. In the ion-implanted material, an increase of interplanar spacing and of the lattice constant is observed [17].

Figure 2 shows the Raman-spectroscopy results for p-n-Si (B).

The position of the band maximum of the starting material (519.4 cm^{-1}) indicates a shift towards lower wave numbers as compared to the classical value for silicon (520 cm^{-1}), which

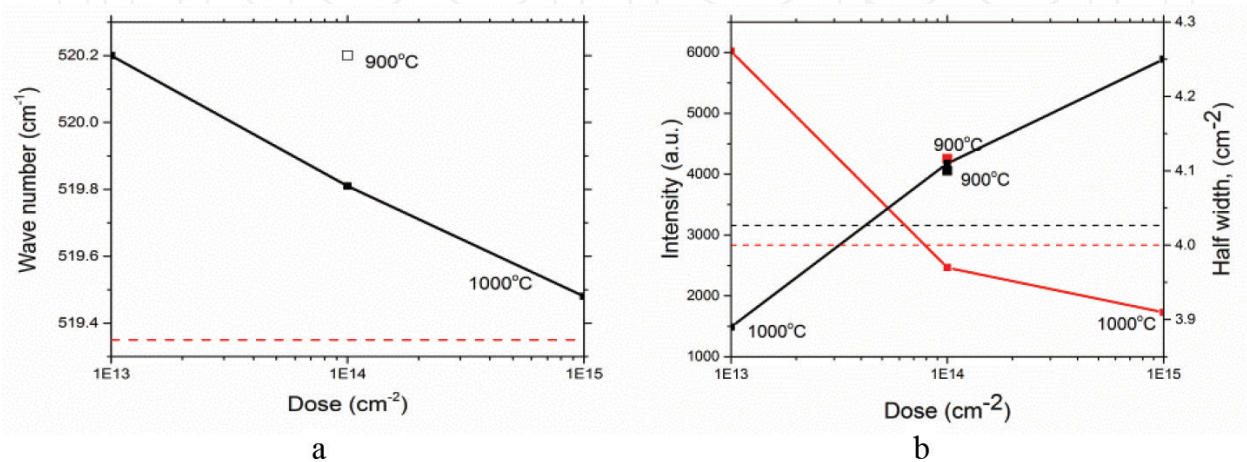| Sample	Lattice parameter, Å	Relative lattice deformation, $\Delta_B/d \cdot 103$	Interplanar spacing, Å	Diffraction line half-width, min	Signal intensity, pulse/s
untreated	5,4304	-	0,91792	14,1	700
II+annealing	5,4311	0,1416	0,91805	17,9	600

Table 1. X-ray diffraction results.

Figure 2. Dose dependence of the Raman spectra parameters: (a) change in the main band position (position of the reference sample maximum is 520 cm^{-1}); (b) intensity (red), half-width (black). The dotted line shows the n-Si data (a,b).

means that n-Si has a near-surface damaged layer. In comparison with the starting material, the maximum of the band for 1×10^{13} cm^{-2} is shifted towards higher values (520.2 cm^{-1}), the intensity becomes twice as much, and the half-width decreases (qualitatively, the same pattern is observed for 1×10^{14} cm^{-2} (annealing at 900°C). Increasing the II dose up to 1×10^{15} cm^{-2} and annealing at 1000°C shifts the band towards smaller wave number values, the intensity decreases, and the half-width increases [19, 21].

Figure 3 demonstrates a typical example of SEM measurements for starting n-Si and p-n-Si(B) annealed at 900 and 1000°C. As follows from these data, the n-Si surface is determined by a homogeneous surface morphology (a). This is also characteristic for the surfaces of the "annealed-only" or "implanted-only" Si. At 900°C, defects of different size appear (b), the amount of which noticeably decreases at 1000°C (c). The samples exhibit a similar behavior at all doses.

Figure 4 shows the diode characteristics typical of the investigated structures, implanted with a dose of 4×10^{14} cm^{-2} and annealed at 900°C (20 min).

Figure 5 illustrates the behavior patterns of leakage currents at different implantation doses for p-n diodes at a voltage of −2 V (a value frequently used in practice). Of particular interest are the data for the Si70 samples: up to the dose of 6×10^{14} cm^{-2} no significant variance in the leakage currents is observed, whereas at higher doses the change exceeds two orders of magnitude. It is remarkable that samples implanted with 1×10^{15} cm^{-2} and annealed at 1000°C
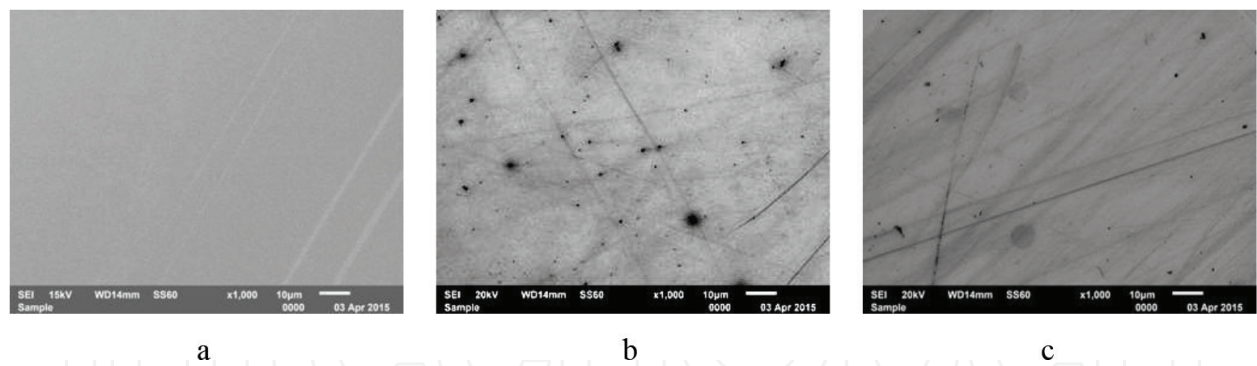
a   b   c

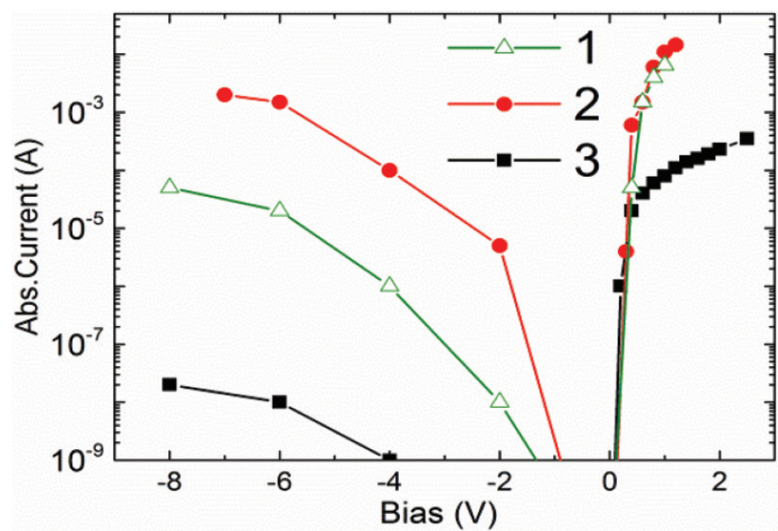**Figure 3.** Surface morphology of the samples in SEM: a—starting n-Si; b—900°C; c—1000°C (×1000) (a, b, c).

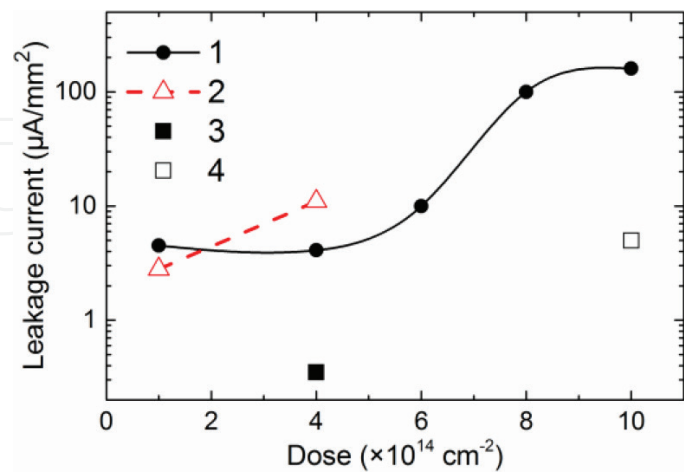**Figure 4.** I-V characteristics of the p-n diodes: (1) Si70; (2) Si10; (3) SOI.

Figure 5. Dependence of the average values of the leakage current density at −2 V on the implantation dose for different samples: (1) Si70, without mesa-etching; (2) Si10 with mesa-etching; (3) SOI with mesa-etching; (4) Si70 after annealing at 1000°C (20 min).

(20 min) exhibit a slight variation of the photoresponse intensity while a drastic (of about 20 times) decrease in the leakage currents is observed. Regarding the Si10 sample, the behavior of the leakage currents can be attributed only to mesa-etched diodes (currents decrease by more than a factor of 80) [22].

Figure 6 shows the IR reflection spectra for the starting n-Si and p-n-Si(B) samples. From these data, the plasma reflection minimum of the untreated silicon wafers is at about 650 cm^{-1}. However, the reflection amplitude is somewhat lower than that corresponding to polished n-Si, probably due to the damaged layer. In the p-n-Si(B) spectra the plasma minimum of the substrate becomes less pronounced and a new minimum appears near 1400 cm^{-1}, which is associated with the presence of a 200–400 nm thick layer with optical parameters different from those of the substrate. The carrier concentration in p-Si is estimated to be of 2×10^{19} cm^{-3}. After implantation and annealing an increase in the band intensity of the Si-O oscillations (1082 cm^{-1}) is observed [19, 21].

Figures 7–13 show the photosensitivity spectra obtained from several samples (Si70, Si10, and SOI) under different conditions of II, annealing, and ion acceleration energies. In addition, for some Si70 samples, the photoresponse spectra were measured at 77°C.

From **Figure 7** it is obvious that the photosensitivity increases for implantation doses of up 6×10^{14} cm^{-2} and then decreases for higher doses. All short-wave infrared (SWIR) spectra exhibit the main maximum corresponding with the wavelength of about 1.8 μm (0.69 eV) and a less pronounced (smoothed) maximum at approximately 1.9 μm (0.65 eV) [20–22].

Figure 8 illustrates an example of the photosensitivity spectra of p-n-Si(B) in the range of 1.5–2.4 μm at 300 K and 77 K for a dose of 8×10^{14} cm^{-2} and annealing at 900°C (20 min). As is evident from the figure, the position of the maxima is practically independent of temperature, whereas their intensity at 77 K is much higher than at 300 K, and the bandwidth is narrowing, especially in the low energy region.

The influence of the annealing temperature on the photoresponse spectra of the Si70 samples implanted with a dose of 1×10^{14} cm^{-2} and annealed at different temperatures was studied in [19]. It was shown that the position of the main peak in the SWIR range, similar to the dose dependence, does not depend on the annealing temperature. The photoresponse intensity is maximal for the annealing temperature of 900°C and minimal for 800°C.

For low resistance silicon (Si10) the same picture is qualitatively observed (**Figure 9**): enhancing the dose from 1×10^{14} to 6×10^{14} cm^{-2} (900°C, 20 min), the photoresponse intensity increases. However, in this case, it is significantly lower for each fixed dose as compared to **Figure 7**. The position of the maxima shifts slightly towards higher energies [22].

Figure 10 shows the influence of the thermal treatment on the photoresponse of p-n diodes (Si10) implanted with a dose of 1×10^{14} cm^{-2} [22].

It is seen from the figure that the PPA impact is more effective. The maximum intensity values (curve 1) approximately correspond to the value obtained at a dose of 4×10^{14} cm^{-2} (curve 2, **Figure 9**). This result requires more detailed studies.

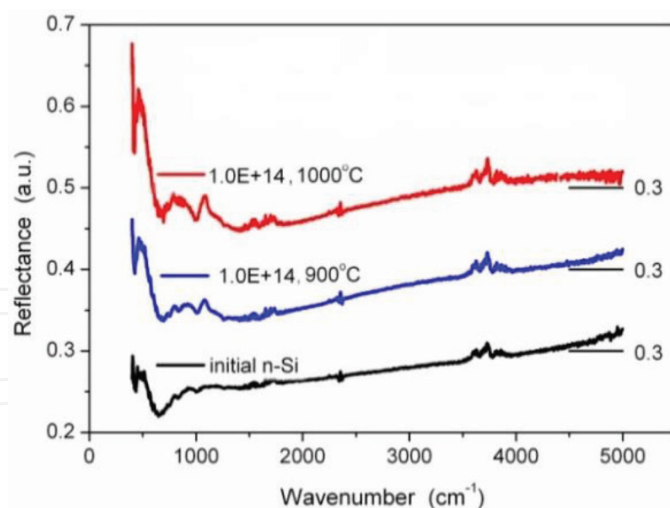**Figure 6.** IR reflection spectra (light incidence angle - 16.5°) of the initial and B implanted (dose 1×10^{14} cm^{-2}) samples annealed at 900 and 1000°C.
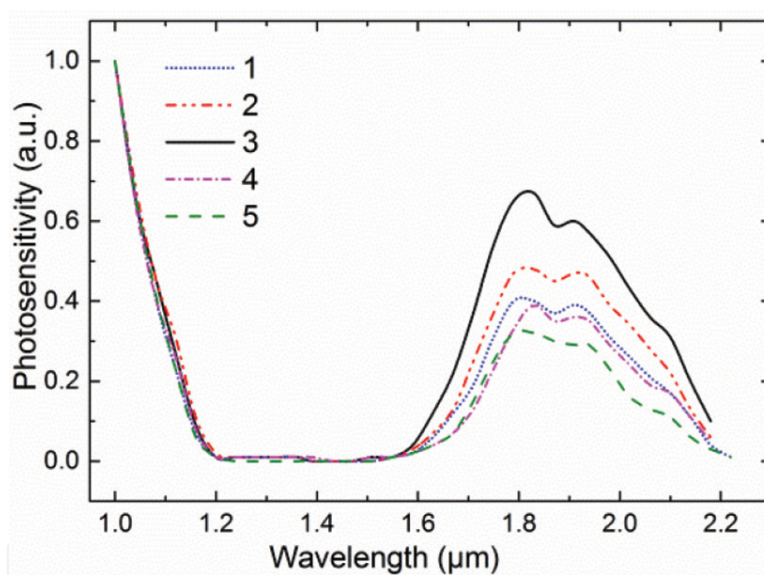

Figure 7. Photosensitivity spectra of the p-n diode (Si70) for different doses: (1) 1×10^{14}; (2) 4×10^{14}; (3) 6×10^{14}; (4) 8×10^{14}; (5) 1×10^{15} cm^{-2}.

In **Figure 11**, a photosensitivity spectrum of the SOI p-n diode is shown. In this case, the character of the dependence differs markedly from the two previous ones: the spectrum is extended, the main maximum is observed at 1.75 μm (0.72 eV), and the second maximum is shifted to the wavelength of 2.04 μm (0.61 eV) [22].

Figure 12 shows the photosensitivity spectra of the p-n-Si(B) structures obtained at an acceleration energy of 32 keV, different doses (1×10^{14} cm^{-2} and 1×10^{15} cm^{-2}) and annealed at 900°C, 20 min.

The comparison of **Figures 12** and **7** shows that the maxima of the photoresponse for 32 keV are approximately 20% higher than the corresponding values for 50 keV.
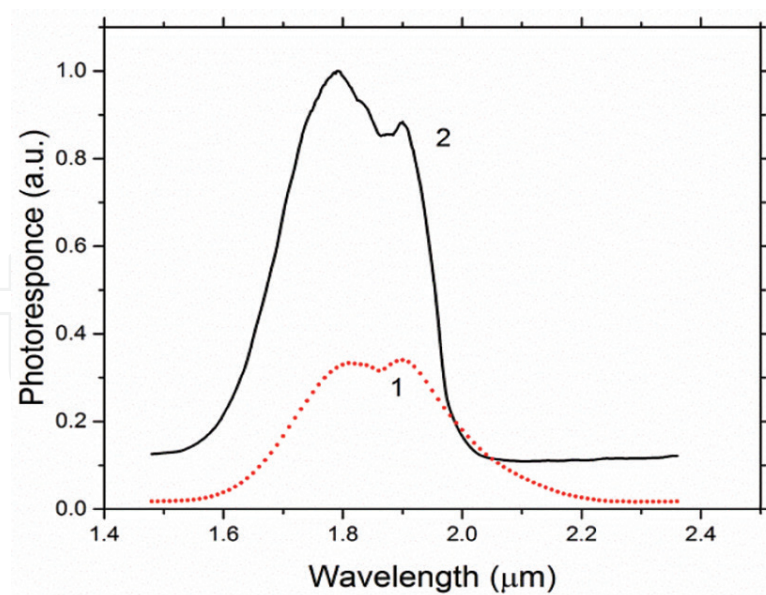
Figure 8. The photosensitivity spectra of p-n diode (Si70) sample implanted with a dose of 8×10^{14} cm^{-2} and annealed at 900°C (20 min): (1) 300 K, (2) 77 K.
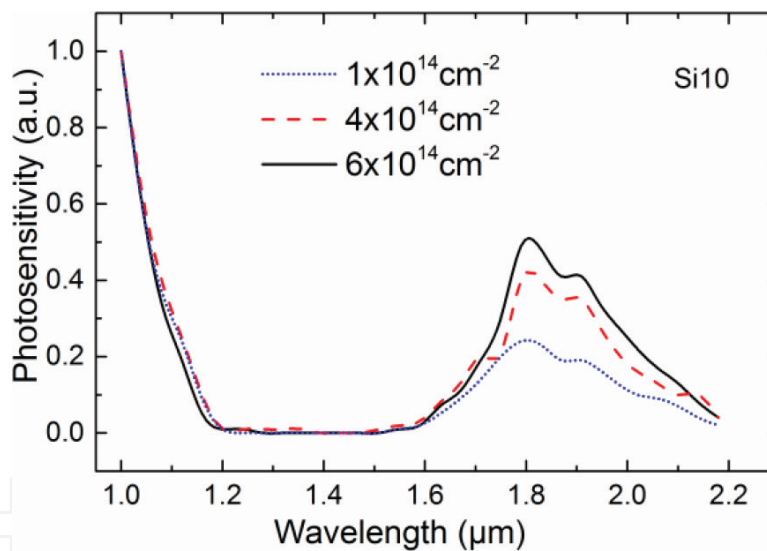

Figure 9. Photosensitivity spectra of the p-n diode (Si10) for different doses: (1) 1×10^{14}; (2) 4×10^{14}; (3) 6×10^{14} cm^{-2}.

Figure 13 shows the photosensitivity vs. the wavelength due to the B$^+$ implantation with the dose of 1×10^{13} cm^{-2} into the untreated material (1) and after the etching of the wafer surface layer to a depth of about 1 μm (2).

As can be seen from the figure, after the etching of the upper layer the photoresponse intensity decreases by a factor of 20, and the main maximum is distinctly less pronounced. The sample with the etched layer behaves in accordance with the proved existence of a threshold dose of 1×10^{14} cm^{-2} to form extended defects.

Figure 14 demonstrates an example of the behavior of the p-n-Si(B) photosensitivity in separate spectral regions within 0.2–4.1 μm. The largest photoresponse corresponds to the red,
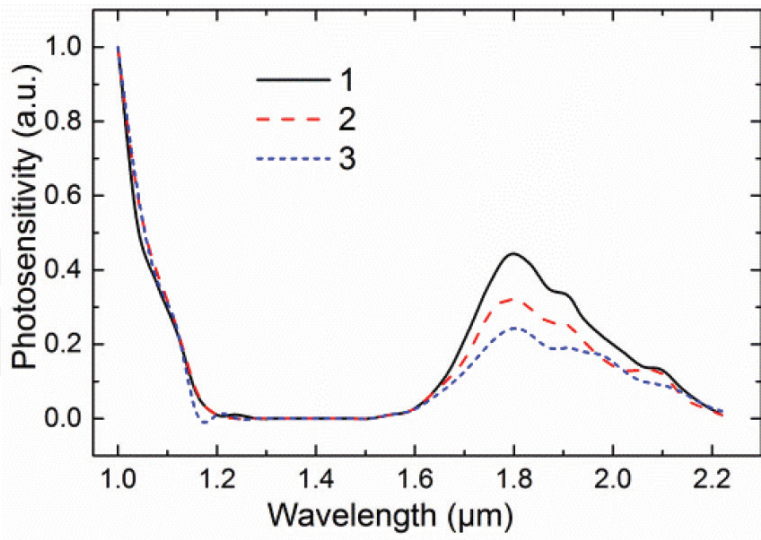
Figure 10. Photosensitivity spectra of the p-n diodes (Si10) for different thermal treatment conditions (dose 1×10^{14} cm^{-2}): (1) PPA at seven 3-s pulses; (2) PPA at three 3-s pulses; (3) in the stationary conditions. Annealing temperature – about 900°C.
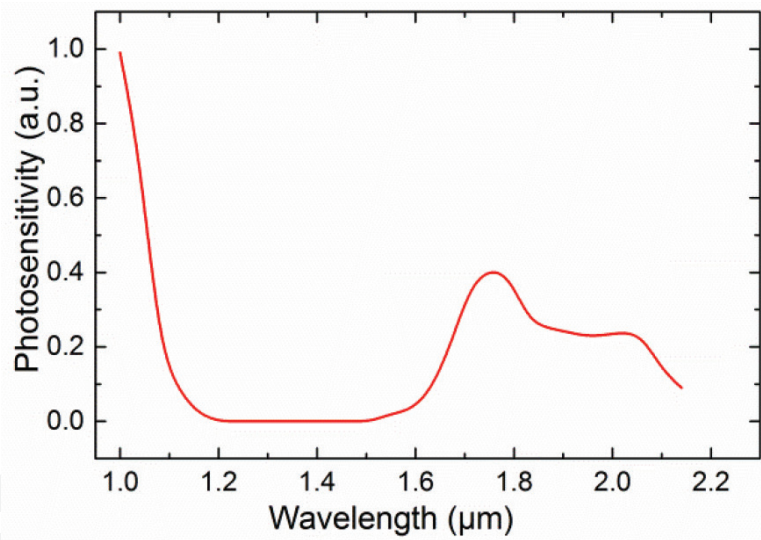

Figure 11. Photosensitivity spectra of the p-n diodes on SOI for the dose of 4×10^{14} cm^{-2}.

near IR and SWIR spectral ranges; a photoresponse is likewise observed in the UV region. It should be noted that, remarkably, areas with zero and negative photosensitivity are detected. These regions are most pronounced for the preselected dose of 6×10^{14} cm^{-2}. The measurement data reported earlier [20, 22] show the dependence of such spectra on the implantation dose and the annealing conditions.

In was shown [21, 22] that in the starting material as well as in n-Si annealed up to 900 and 1000°C or B$^+$ implanted without annealing only silicon is detected within the SEM sensitivity
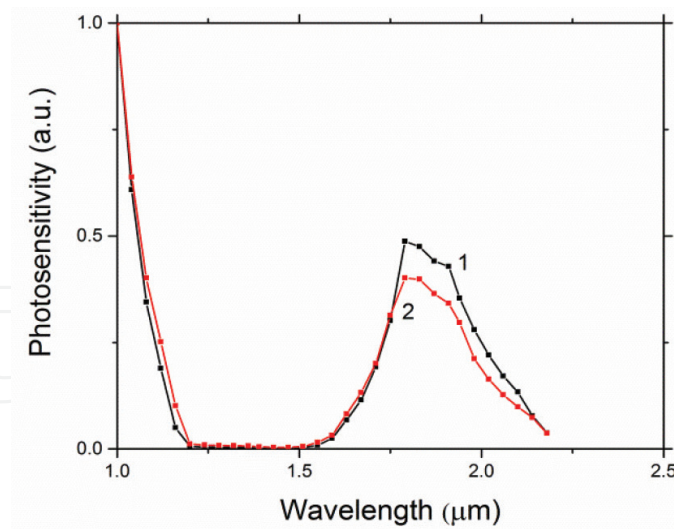
Figure 12. The photosensitivity spectra of the p-n diodes (Si70) obtained at an acceleration energy of 32 keV and different doses: $1–1 \times 10^{14}$ cm^{-2}; $2–1 \times 10^{15}$ cm^{-2} (annealing - 900°C, 20 min).
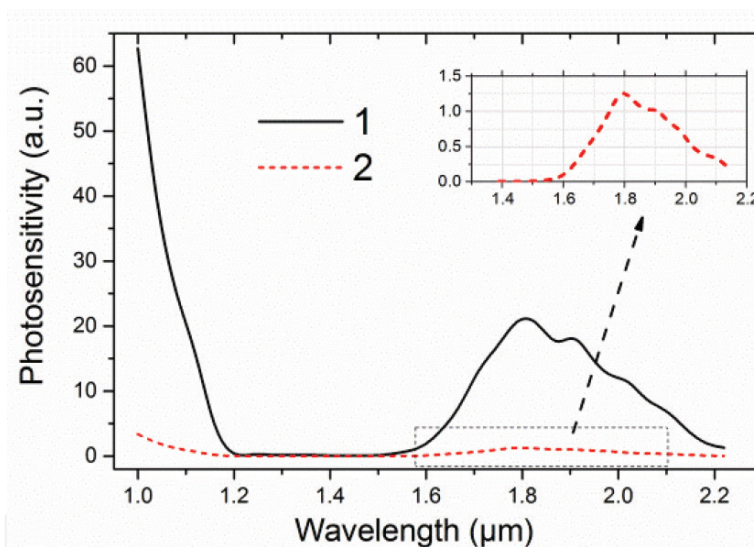

Figure 13. Photosensitivity spectrum for p-n diode (Si70) samples implanted with a dose of 1×10^{13} cm^{-2}: (1) the substrate surface is not etched; (2) the surface etched to a depth of about 1 μm; in the upper right corner the dependence of 2 is presented in an enlarged scale.

range. A completely different picture is obtained for the p-n-Si(B) structures (**Figure 15a**): a surprisingly high content of C and O is detected in the samples, depending on the implantation and annealing conditions. For comparison, **Figure 15b** shows the dependencies of the integrated photosensitivity on similar technological conditions.

The detection of C and O after implantation and annealing indicates the gettering of these impurities via the specimen surface. From the concentration levels it is quite likely to assume
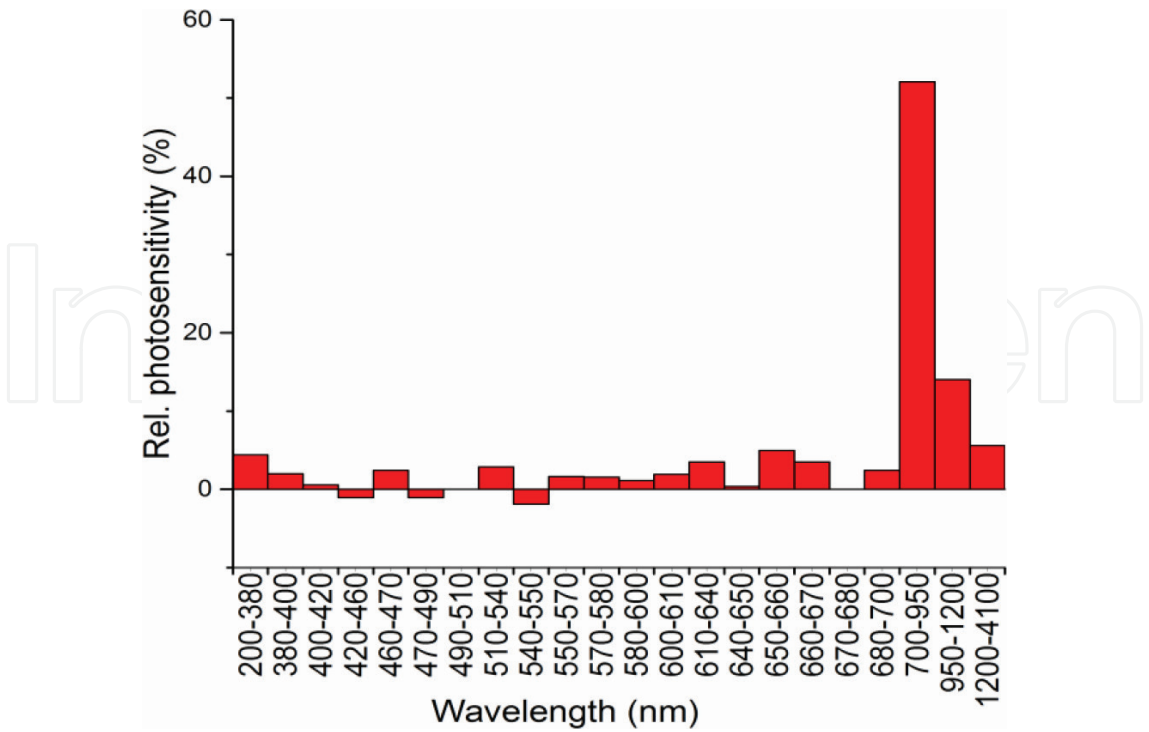
Figure 14. Spectral dependence of the integral relative photosensitivity for the p-n-Si(B) structure at the dose of 6×10^{14} cm^{-2}.

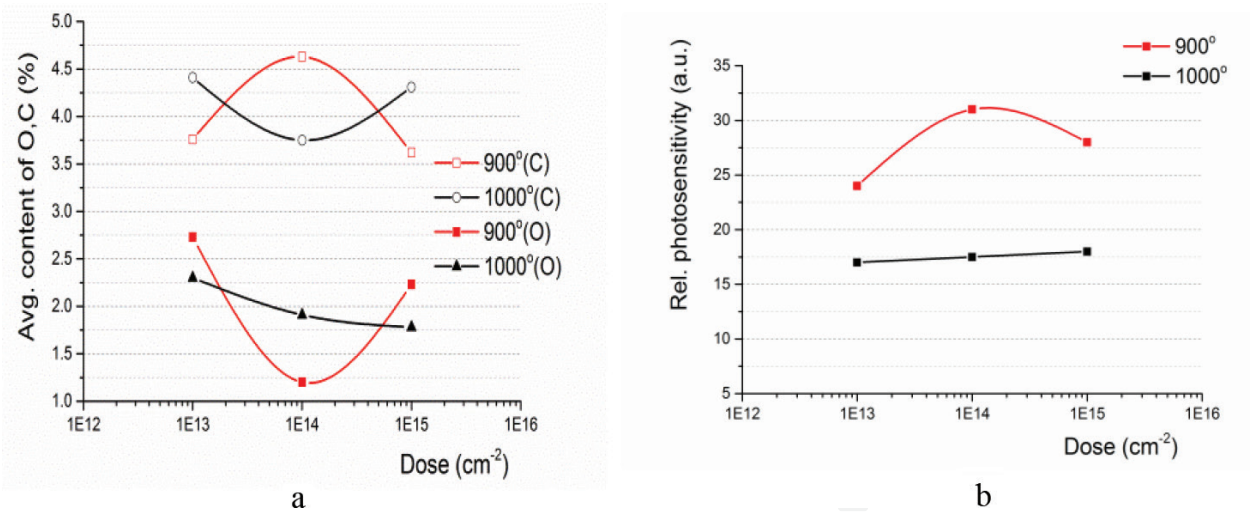**Figure 15.** Dose and annealing temperature dependences of: (a) carbon and oxygen content; (b) relative integrated photosensitivity (a, b).

that oxygen has the most critical effect on the formation of defects responsible for the photosensitivity: the lower its content, the higher the photoresponse at both annealing temperatures applied. The C content, though higher than that of O in our case, appears to be less critical.
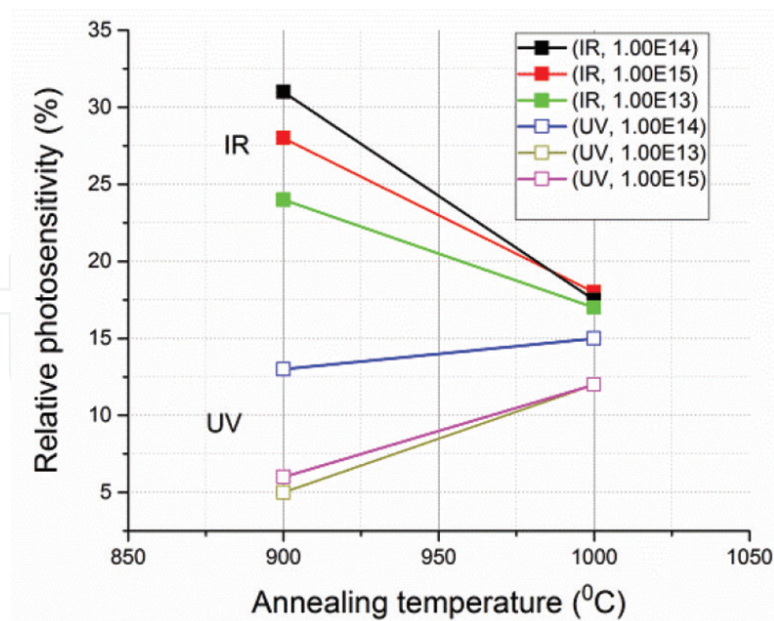
Figure 16. Relative integrated photoresponse for different doses and annealing temperatures in the ranges: UV—0.25–0.40μm; IR—1.0–4.1 μm.

Figure 16 illustrates the presence of a pronounced photoresponse in the UV range for different doses and annealing temperatures, even under EMR of weak intensity. For comparison, similar dependencies for the IR range are also displayed [21].

As indicated by the figure, the annealing temperature has quite a different effect on the photosensitivity in the UV and IR spectral ranges. For both cases the maximum photoresponse is accounted for a dose of 1×10^{14} cm^{-2}, for the UV it slightly depends on the annealing temperature. The behavior of the UV photoresponse for the two other doses applied is almost the same.

It is interesting to note that, in the 1000°C annealing temperature regime, the photoresponse signals in the IR range are practically identical for all three implantation doses.

4. Discussion

From our results of studies of n-Si wafers using Raman (**Figure 2**) and IR (**Figure 6**) spectroscopy we conclude that there is strain in the crystal structure due to the damaged near-surface layer of the material [19, 21]. According to some literature data [23], such a distorted layer can range from hundreds of nanometers to tens of microns, and in our case [21], within the measurement accuracy, it has a depth of several hundred nanometers. Obviously, this layer affects the variance in the characteristics of the material when doped by II. X-ray diffraction data suggest (**Table 1**) that there is no complete restoration of the structure after the II even with an annealing temperature of up to 1000°C.

It is established (**Figures 7–12**) that for all materials under the II and annealing regimes applied in our research work, the photosensitivity is observed in p-n-Si(B) within the wavelength range of 1.5–2.2 µm with two maxima of about 1.8 µm (main) and 1.9 µm (less pronounced) for Si70 and Si10. For SOI they are shifted towards lower and higher wavelengths, respectively.

In an attempt to explain the observed effects, it seems reasonable to rely on a complex physical mechanism indicating that the formation of extended defects with DL in the bandgap, occurs mainly in the damaged layer of the starting material. This assumption is supported by the following experimental results. **Figure 13** illustrates that the presence of the damaged layer can shift the "threshold" conditions of the formation of extended defects from a dose of 1×10^{14} cm^{-2} to 1×10^{13} cm^{-2}. Decreasing the ion acceleration energy from 50 to 32 keV (**Figure 12**) or replacing stationary regimes by PPA (**Figure 10**) leads to a marked increase in the intensity of the photoresponse with II doses unchanged. Apparently, the energy change leads to the change in the size and density of extended defects [10], and during PPA the shift of the p-n junction towards the more distorted near-surface region takes place.

From common knowledge on the formation/transformation of defects in B$^+$ implanted n-Si at annealing temperatures of 900 and 1000°C that we essentially applied in our studies, it is expected that point defects, small clusters and defects road-like{311} should be completely annealed. However, during the annealing process, defects {311} form dislocation loops of various configurations that persist up to 1000°C and above. Regardless of the doses for Si70 and Si10, some defects form DL in the bandgap with activation energies of about 0.7 and 0.65 eV. The corresponding maxima (main and smoothed) in the photosensitivity spectra are characterized by their intensity that differ with respect to their dose and annealing dependency. The increase in the photosensitivity intensity up to the dose of 6×10^{14} cm^{-2} is associated with the growing concentration of these defects. Increasing the dose further up to 1×10^{15} cm^{-2} the number of electrically active defects decreases and new defects appear that do not affect the photoelectric properties of the material. A sharp intensity increase and a marked band half-width decrease at 77 K indicate an increase in the occupation of DL formed by defects responsible for the photosensitivity (**Figure 8**). Altogether, it is reasonable to assume that, under these implantation and annealing conditions, the electrically active defects are generally evolving dislocation loops [9, 10].

The behavior of leakage currents (**Figure 5**) at high doses of II and annealing at 900°C can be described by the formation of new dislocation-type defects, a part of which leads to generation-recombination processes in the space charge region and affects the reverse current in the diode. At 1000°C these defects are annealed, reducing the leakage currents by a factor of about 20.

The understanding of the defect formation mechanism becomes even more complicated due to the observed correlation between the content of carbon and oxygen impurities in the surface layer and the IR photoresponse at different doses and annealing regimes (**Figure 15**). At this stage, we can only assume that the effect of oxygen on the defects responsible for the photosensitivity is much stronger than that of carbon: for oxygen the shape of the dose dependence curve at 900°C exhibits an opposite behavior to that of the photoresponse at the same temperature. In addition, after implantation and annealing, a change in the band intensity of

the Si-O oscillations (1082 cm^{-1}) with increasing annealing temperature from 900 to 1000°C is observed (**Figure 6**). The role of carbon might rather be indirect, since an increase in the carbon content reduces the concentration of gettered oxygen. The negative effect of oxygen on the photoresponse intensity is also reported in [24]. If annealing occurs at 1000°C, all these processes are much less pronounced.

Another interesting effect is observed on the integrated photosensitivity spectra (**Figure 14**) at EMR energies exceeding the bandgap value of silicon - the appearance of areas of zero and negative photosensitivity. The light absorption coefficient in this spectral region $\alpha \approx (1–5) \times 10^4$ cm^{-1} and the corresponding absorption depth is of the order of 1 μm. The appearance of areas with negative photoresponse depends on the spectral composition of the incident light, and the intensity at the same annealing temperature (900, 20 min) depends on the II dose, increasing from 1×10^{14} to 6×10^{14} cm^{-2}. The observed negative photosensitivity is apparently due to the presence of surface levels in p-n-Si(B) structures, which are trapping centers of the majority charge carriers. The population of these levels depends on the spectral composition of the light, and their concentration and depth are determined by the processing conditions of ion doping.

It is evident from the data of **Figure 16** that the mechanisms of photoresponse in SWIR and UV regions are completely different. At high energies of the EMR in the UV region, the absorption processes must occur in the surface layer. Most likely, the intensity of the UV photoresponse should increase with the annealing temperature due to a decrease in the concentration of trap centers.

The share of the photosensitivity in the SWIR is estimated to be up to 9%, whereas in the UV region it is up to 7% of the total photosensitivity in the range of 200–4100 nm (**Figure 14** and [18, 19, 21]).

In general, the interpretation of a number of obtained data and the underlying physical mechanisms requires additional clarification.

It is important to note that the technology itself and the measurement results are well reproducible. Hence, using the damaged layer in the starting material, it is possible to realize the controllable photoelectrical properties of p-n structures and propose this process as an innovative approach to the development of SWIR array photodetectors. In this respect, high-resistance n-Si samples implanted with a dose of B$^+$ 6×10^{14} cm^{-2} and annealed at 900°C (20 min) may find practical application as SWIR pixel arrays. Based on SOI structures, a quasi-planar array can be developed, especially for those cases where a relatively weak output signal is "compensated" by low leakage currents. The development of a UV detector technology is also envisaged.

5. Conclusions

The results of the recent original studies in the field of purposeful modification of the photoelectrical properties of n-Si due to B$^+$ ion implantation are supplemented with new data, summarized and analyzed.

The starting material was wafers of single-crystalline n-Si with different resistivity (70 and 10 Ohm·cm) and a SOI structure as well. For the fabrication of the p-n-Si(B) structures, ion implantation of B^+ was applied with doses of 1×10^{13}, 1×10^{14}, 4×10^{14}, 6×10^{14}, 8×10^{14} and 1×10^{15} cm^{-2} and acceleration energies of 50 and 32 keV with subsequent annealing in stationary (800, 900 and 1000°C, 20 min) and pulse-photon regimes.

The structural characteristics of the samples were studied by X-ray diffraction, Raman and IR spectroscopy. The surface properties of the samples were analyzed by SEM. The photoconductivity (photoresponse) was studied on a monochromator in the SWIR region (1.2–2.5 μm) and on a special setup that allows samples to be illuminated with a "packet" of waves in the range of 0.2–4.1 μm.

In the studied structures, a pronounced photosensitivity was detected in the range of 1.5–2.2 μm with two maxima of about 1.8 μm (main) and 1.9 μm (less pronounced) for Si70 and Si10. For SOI they are shifted towards lower and higher wavelengths, respectively. A pronounced photoresponse is detected in the UV region (0.25–0.40 μm).

A well-defined correlation between the structural, electrical and photoelectrical properties in SWIR and UV regions on the one hand, and implantation and annealing regimes as well as the content of C and O impurities on the other hand, is demonstrated. In the starting material, a damaged near-surface layer with a thickness of hundreds of nanometers was found to have a significant effect on the results obtained.

The effects observed in the SWIR range are discussed in terms of the formation/ transformation of extended defects with DL (0.7 and 0.65 eV for Si70 and Si10, 0.72 and 0.61 eV for SOI) in the material, most likely dislocation loops. The photoresponse intensity in the UV range seems to be associated with a change in the concentration of trap centers in the near-surface layer of p-n-Si(B) structures. The regions with a negative photoresponse observed on the integrated photosensitivity spectra depend on the spectral composition of the incident light. We attribute this effect to the presence of trapping centers of the main charge carriers in the near-surface layers of the sample.

Taking into account that the technology itself and the measurement results are well reproducible for different monocrystalline n-Si, it is evident that boron implantation permits controlled modification of photoelectrical properties of the material.

The results obtained can be used to develop SWIR pixel and quasi-planar arrays and UV detectors as well.

Acknowledgements

Author details

Nina Khuchua[1]*, Marina Tigishvili[2], Nugzar Dolidze[2], Zurab Jibuti[2], Revaz Melkadze[1] and Roland Diehl[3]

*Address all correspondence to: ninakhuchua@mail.ru

1 RPC "Electron Technology", Institute of Applied Semiconductor Technology, Iv.Javakhishvili Tbilisi State University, Tbilisi, Georgia

2 Institute of Micro- and Nanoelectronics, Tbilisi, Georgia

3 Fraunhofer Institute for Applied Solid-State Physics (IAF), Freiburg im Breisgau, Germany

References

[1] Milvidskii M, Chaldyshev V. Nanoscale atomic clusters in semiconductors as a new approach to formation of materials properties. Fizika i Tekhnika Poluprovodnikov. 1998;**32**:513-522

[2] Kotov V, Klindukhov V, Cherepasgkin I. Modification of the silicon structure and optical properties by electric pulse treatment. Nano-i Microsistemnaya Tekhnika. 2000;**3**:8-10

[3] Vavilov V, Chelyadinsky A. The ion implantation of impurities crystalline Si single crystals: The efficiency of this method and the radiation damage. Uspekhi Fizicheskikh Nauk. 1995;**165**:347-358. DOI: 10.2267/UFNr.0165.199503g.0347

[4] Libertino S, La Magna A. Damages formation and evolution in ion-implanted crystalline Si. In: Bernas H, editor. Material Science with Ion Beams. Topics in Applied Physics. Vol. 116. Berlin Heidelberg: Springer-Verlag; 2010. pp. 147-212. DOI: 10. 1007/978-3-540-88789-8-6

[5] Casalino M. Near-infrared sub-bandgap all-silicon photodetectors: A review. International Journal of Optics and Applications. 2012;**2**:1-16. DOI: 105923/j.optics.2012201.01

[6] Lastkin V, Gavrushko V, Ionov A. An improves silicon UV-photodiode obtained by As implantation. Elektronika: Science, Technology, Business. 2010;**2**:72-73

[7] Eichler S, Gebauer J, Börner F, Polity A, Krause-Rehberg R, Wendler E, Weber B, Wesch W, Borner H. Mint: Defects in silicon after B+ implantation: A study using a positron-beam technique, Rutherford backscattering, secondary neutral mass spectroscopy and infrared absorption spectroscopy. Physical Review B. 1997;**56**:1393-1403. DOI: 10.1103/PhysRevb.56.1393

[8] Feklistov K, Fedina L, Cherkov A. Mint: Boron precipitation in Si at high implantation dose. Fizika i Tekhnika Poluprovodnikov. 2010;**44**:302-305

[9] Duguay S, Philippe T, Cristiano F, Blavette D. Direct imaging of boron segregation to extended defects in silicon. Applied Physics Letters. 2010;**97**:242104-1-242104-3. DOI: 10.1063/1.3526376

[10] Milosavljević M, Shao G, Lourenco M, Gwillian R, Homewood K. Engineering of boron-induced dislocation loops for efficient room-temperature silicon light-emitting diodes. Journal of Applied Physics. 2005;**97**:073512-1-073512-7. DOI: 10.1063/1.1866492

[11] Sobolev N, Emelianov A, Shek E, Vdovin V. Influence of post-implantation annealing on the properties of silicon light-emitting diodes obtained by boron implantation in n-Si. Physika Tverdogo Tela. 2004;**46**:39-43

[12] Cheladinski A, Komarov Ph. Defect-impurity engineering in implanted silicon. Uspekhi Fizicheskikh Nauk. 2003;17:8-46. DOI: 10.3367/UFNr.0173.200308b.0813

[13] Válek L, Śik J. Defect engineering during Czochralski crystal growth and silicon wafer manufacturing. In: Kolesnikov N, editor. Modern Aspects of Bulk and Thin Film Preparation. InTech: Rijeka; 2012. pp. 43-70

[14] Usami A, Katayama M, Mint WT. Diode characteristics and residual deep- level defects of p$^+$-n abrupt junctions fabricated by rapid thermal boron implanted silicon. Semiconductor Science Technology. 1987;**2**:83-87

[15] Vyzhigin Y, Sobolev N, Gresserov B, Shek E. Influence of the thermal treatment temperature on the formation of deep-level center. Fizika i Technika Poluprovodnikov. 1991;**25**:1324-1331

[16] Gavrushko V, Ionov A, Lastkin V. Analysis of the influence of technological parameters and a type of photodetectors on their photosensitivity in the UV spectral region. In: Proceedings of The 6-th All-Russian Youth School "Materials of Nano- Micro- and Optoelectronic Technology: Physical"

[17] Tigishvili M, Gapishvili N, Gulyaev R, Jibuti Z, Dolidze N, Khuchua N, Melkadze R. Defect engineering in the silicon p-n junction technology. Georgian Engineering News. 2013;**68**:75-79

[18] Khuchua N, Dolidze N, Gapishvili N, Gulyaev R, Jibuti Z, Melkadze R, Tigishvili M. Technology of semiconductor materials sensitive to different regions of the electromagnetic radiation spectrum. Nanotechnology Perceptions. 2014;**4**:91-99

[19] Tigishvili M, Khuchua N, Melkadze R, Dolidze N, Gapishvili G, Jibuti Z, Dovbeshko G, Romanyuk V. Semiconductor material with new optical properties for infrared and ultraviolet photodetectors. In: Proceedings of the 2nd International Conference on Modern Technologies and Methods of Inorganic Materials Science; 20-24 April 2015; Tbilisi Georgia. Tbilisi: Edition of National Academy of Sciences of Georgia; 2015. pp. 288-295

[20] Dolidze N, Jibuti Z, Tigishvili M, Khuchua N, Melkadze R, Gapishvili N. Effect of light spectral composition on photoelectric properties of ion doped silicon. In: Proceedings of the International Conference on Advanced Materials and Technologies; 21-23 October

2015; Tbilisi, Georgia. Tbilisi: Edition of National Academy of Sciences of Georgia; 2015. pp. 63-67

[21] Khuchua N, Tigishvili M, Melkadze R, Dolidze N, Gapishvili N, Jibuti Z, Dovbeshko G, Romanyuk V. Defect formation in ion-implanted Si-approach to controlled semiconductor optical properties. In: Proceedings of the International Conference on Gettering Defect Engineering in Semiconductor Technology XVI; 20-25 September 2015; Bad Staffelstein, Germany. Solid State Phenomena. 2016;**242**:374-379. DOI: 10.4028/www.scientific.net/SSP.242.374

[22] Tigishvili M, Khuchua N, Gapishvili N, Sakharova T, Dolidze N, Jibuti Z, Peradze G, Melkadze R. Impact of damages in monocrystalline n-Si on material photosensitivity. In: Proceedings of the International Conference on Gettering Defect Engineering in Semiconductor Technology XVII; 1-6 October 2017; Lopota Resort, Georgia. Physica Status Solidi. 2017;**C14**:1700094-1-1700094-6. DOI: 10.1002/ppsc.201700094

[23] Mikhajlov A, Belov A, Korolyev D, Timofeeva A, Vasilyev B, Bobrov A, Pavlov D, Tetelbaum D, Shek E. Effect of ion doping on photoluminescence of silicon originated from dislocations formed by Si^+ ion implantation. Physika i Tekhnika Poluprovodnikov. 2014;**48**:212-216

[24] Blynski V, Bozhatkin O, Holub E, Lemeshevskaya A, Shvedov S. Effect of preliminary annealing of silicon substrates on the spectral sensitivity of photodetectors in bipolar integrated circuits. Journal of Applied Spectroscopy. 2010;**77**:478-481